Nonperturbative and perturbative parts of energy eigenfunctions: A three-orbital schematic shell model

Wen-ge Wang
Department of Physics, Southeast University, Nanjing 210096, China
(Received 1 May 2001; revised manuscript received 23 October 2001; published 27 February 2002)

We study the division of components of energy eigenfunctions, as the expansion of perturbed states in unperturbed states, into nonperturbative and perturbative parts in a three-orbital schematic shell model possessing a chaotic classical limit, the Hamiltonian of which is composed of a Hamiltonian of noninteracting particles and a perturbation. The perturbative parts of eigenfunctions are expanded in a convergent perturbation expansion by making use of the nonperturbative parts. The division is shown to have the property that, when the underlying classical system is chaotic, the statistics of the components of the nonperturbative parts whose relative localization length are close to 1 is in agreement with the prediction of random-matrix theory. When the underlying classical system is mixed, main bodies of most of the eigenfunctions are found to occupy parts of their nonperturbative regions, with some of the rest of the eigenfunctions being ''ergodic'' in their nonperturbative regions due to avoided level crossings. In case of the classical system being chaotic, most of the eigenfunctions are found ''ergodic'' or almost ''ergodic'' in their nonperturbative regions. Numerical results show that the average relative localization length of nonperturbative parts of eigenfunctions is useful in characterizing the behavior of the quantum system in the process of the underlying classical system changing from a mixed system to a chaotic one.

DOI: 10.1103/PhysRevE.65.036219 PACS number(s): 05.45.−a

I. INTRODUCTION

Energy eigenstates in conservative quantum systems with chaotic classical limits have attracted lots of attention in the past more than two decades in the field of the so-called quantum chaos (see, e.g., [1–4]). Still there are some properties of energy eigenfunctions in classically chaotic systems that have not been studied well. For energy eigenfunctions expressed in configuration space that are sufficiently irregular and ''ergodic,'' it has been found that the statistics of wave function probability intensities is in agreement with the prediction of random-matrix theory [5,6]. However, for eigenfunctions taken as the expansion of perturbed states in unperturbed states, the statistics of their components has been found deviating from the prediction of random-matrix theory (RMT), when the underlying classical systems are chaotic (see, e.g., [7]). This is because such eigenfunctions usually have decaying tails that can be described by perturbation theory (see, e.g., [8,9]), but not by RMT [2,10,11]. The statistics cannot be made in agreement with the prediction of RMT by simply subtracting components below some threshold, which would make the number of components below the threshold zero. The problem is how to separate the decaying tails described by perturbation theory from the other parts of eigenfunctions analytically. This problem is also of relevance to the problem of localization in conservative quantum systems [12,13]. Recently, it has been found that dynamical localization can appear not only in time-dependent systems [14], but also in conservative systems [15–18], the mechanism of which is still unclear.

Quantum systems whose classical limits are in transition from integrability to chaos are of particular interest in the field of quantum chaos. Among them, the most intensely studied one is probably the hydrogen atom in a magnetic field [19]. In the meantime, there are also many other systems that have attracted lots of attention (see, e.g., [20–24]). For mixed systems described in configuration space, interesting progress has been achieved in the understanding of their statistical properties, e.g., by assuming independent sequences of eigenstates from different phase-space components, statistical properties of transition matrix elements have been found related to the mixed character of phase space [25–27]. However, there are still some interesting problems that have not been investigated well. For example, for eigenfunctions taken as the expansion of perturbed states in unperturbed ones, whether or not the scope of the main bodies of the eigenfunctions in a given energy region can be estimated to some extent by using the Hamiltonian matrix elements directly, without diagonalizing the Hamiltonian matrices. For a classical system in a transition from integrability to chaos, the degree of the destruction of integrability can be measured by μ, the fraction of chaotic volume in phase space. But, for quantum systems, only parameters of interpolation are known, e.g., the parametrization of Brody *et al.* [28], Berry and Robnik [29], and Izrailev [30], although, in principle, there should exist some parameters directly related to properties of quantum systems that can be used to characterize the process.

A clue to possible solutions to the above problems comes from a so-called generalization of Brillouin-Wigner perturbation theory (GBWPT), which was proposed in the study of a model system with a bandlike structure of the Hamiltonian matrix [23]. In ordinary perturbation theories, such as the Rayleigh-Schrödinger perturbation theory and the Brillouin-Wigner perturbation theory, when unperturbed systems have no degenerate or quite close lying levels, components of an eigenfunction, except the largest one, are expressed in a perturbation expansion by making use of the largest component. As well known, when the largest component does not dominate, i.e., when there are other large components, the perturbation expansion usually diverges. The basic idea underlying

the GBWPT is that, when perturbation is not weak and an eigenfunction have more than one large components, in stead of the largest component, one can make use of *more than one suitably chosen components* to expand the other components in a convergent perturbation expansion. The smallest number of components made use of in the convergent perturbation expansion gives a natural analytical division of the eigenfunction into two qualitatively different parts. Such a division is useful in the study of the structure of eigenfunctions, for example, it can be compared with the division of eigenfunctions into central parts and tails found numerically. For the so-called Wigner-band random-matrix (WBRM) model [31] consisting of band random matrices with increasing diagonal elements, it has been found that tails of eigenfunctions are on average associated with the parts of eigenfunctions expanded in a convergent perturbation expansion, termed the perturbative parts of eigenfunctions, with the other parts termed the nonperturbative parts of eigenfunctions [13]. The division is also useful in approximate calculation of eigenfunctions by truncated matrices, since it can be estimated before the exact energies are known [32].

In this paper, we will give an investigation of the relationship between the two divisions of eigenfunctions mentioned above in a dynamical system with a chaotic classical limit. When the two divisions are relevant to each other, it would be natural to study statistical properties of the nonperturbative parts of eigenfunctions, to see whether they can be related to the prediction of RMT. As well known, on the one hand, perturbed states of a chaotic system usually have wide distribution over unperturbed states of regular systems, on the other hand, a wide distribution of eigenfunctions does not necessarily mean that the investigated system is chaotic. Similarly, we expect there may exist some relationship between statistical properties of nonperturbative parts of eigenfunctions and the prediction of RMT, only when the investigated system is chaotic and the reference system is regular. Also in this sense, we are to study properties of eigenfunctions with respect to their nonperturbative parts, when the underlying classical system undergoes a crossover from integrability to chaos.

The dynamical model we will employ in this paper is a three-orbital schematic shell model [33], in short, the LMG (Lipkin-Meshkov-Glick) model or Lipkin model, whose classical counterpart can be chaotic when perturbation is strong enough [7,23,34]. The definition of perturbative and nonperturbative parts of eigenfunctions used in the case of the WBRM model [13] is not suitable for the Lipkin model. In Sec. II, we will propose a more general definition for them, after a recall of the main results of the GBWPT. With the proposed definition, it will be shown numerically that the statistics of the nonperturbative parts of eigenfunctions that are sufficiently ergodic is in agreement with the prediction of RMT. Section III will be devoted to a numerical study of properties of eigenfunctions with respect to their nonperturbative regions, when the underlying classical system undergoes a transition from integrability to chaos. In particular, the average relative localization length of nonperturbative parts of eigenfunctions will be studied, in comparison with the classical parameter μ, the Brody parameter β, and the ordinary localization length. Conclusions and discussions will be given in Sec. IV.

II. DEFINITION OF NONPERTURBATIVE PARTS OF EIGENFUNCTIONS

A. Generalization of Brillouin-Wigner perturbation theory

Before the discussion of the definition of nonperturbative parts of eigenfunctions, let us first recall the main results of the GBWPT. Consider a Hamiltonian of the form $H(\lambda)=H_0+\lambda V$, where H_0 is an unperturbed Hamiltonian and λV represents a perturbation with λ being a running parameter. The eigenstates of the Hamiltonians $H(\lambda)$ and H_0 are denoted by $|\alpha\rangle$ and $|k\rangle$, respectively,

$$H(\lambda)|\alpha\rangle=E_\alpha(\lambda)|\alpha\rangle, \quad H_0|k\rangle=E_k^0|k\rangle, \tag{1}$$

with the labels $\alpha,k=1,2,\ldots$ in energy order. In the GBWPT, for each perturbed state $|\alpha\rangle$, the set of unperturbed states $|k\rangle$ is divided into two subsets, denoted by S_α and $\bar{S}_\alpha$, and consequently the perturbed state itself is divided into two parts, $|\alpha_s\rangle\equiv P_{S_\alpha}|\alpha\rangle$ and $|\alpha_s^-\rangle\equiv Q_{\bar{S}_\alpha}|\alpha\rangle$, by two projection operators

$$P_{S_\alpha}=\sum_{|k\rangle\in S_\alpha}|k\rangle\langle k|, \quad Q_{\bar{S}_\alpha}=\sum_{|k\rangle\in \bar{S}\alpha}|k\rangle\langle k|=1-P_{S_\alpha}. \tag{2}$$

It can be shown that $|\alpha_s^-\rangle$ can be expanded in a convergent perturbation expansion by making use of $|\alpha_s\rangle$,

$$|\alpha_s^-\rangle=T_\alpha|\alpha_s\rangle+T_\alpha^2|\alpha_s\rangle+\cdots+T_\alpha^n|\alpha_s\rangle+\cdots, \tag{3}$$

when the condition

$$\lim_{n\to\infty}\langle\alpha|(T_\alpha^\dagger)^nT_\alpha^n|\alpha\rangle=0 \tag{4}$$

is satisfied, where

$$T_\alpha=\frac{1}{E_\alpha-H_0}Q_{\bar{S}_\alpha}\lambda V. \tag{5}$$

The condition (4) can be satisfied, when the set S_α is large enough, e.g., as an extreme case, when $\bar{S}_\alpha$ has one unperturbed state $|k\rangle$ only with $\langle k|V|k\rangle=0$. However, with increasing S_α, the information on properties of eigenfunctions supplied by the GBWPT will be reduced.

As shown in Ref. [13], the condition (4) is, in general, equivalent to the requirement that $|\lambda u_{\alpha\nu}|<1$ for all the states $|\nu_\alpha\rangle$, where $|\nu_\alpha\rangle$ and $u_{\alpha\nu}$ are (right) eigenvectors and eigenvalues of

$$U_\alpha\equiv Q_{\bar{S}_\alpha}V\frac{1}{E_\alpha-H^0}Q_{\bar{S}_\alpha}, \tag{6}$$

which is an operator in the subspace spanned by unperturbed states in $\bar{S}_\alpha$. Only when $\langle\nu_\alpha|Q_{\bar{S}_\alpha}V|\alpha\rangle=0$, can $|\lambda u_{\alpha\nu}|$ be larger than or equal to 1 under the condition (4), which is

quite exceptional and not to be discussed here. As a result of $|\lambda u_{\alpha\nu}|<1$, the condition (4) can be replaced by

$$\lim_{n\to\infty}\langle\phi|(T_\alpha^\dagger)^n T_\alpha^n|\phi\rangle=0, \tag{7}$$

with $|\phi\rangle$ being an arbitrary state. For each $|j\rangle$ in a set $\overline{S_\alpha}$ satisfying Eq. (4), expanding the state $Q_{\overline{S}_\alpha}\lambda V|\alpha_s\rangle$ in the states $|\nu_\alpha\rangle$, $Q_{\overline{S}_\alpha}\lambda V|\alpha_s\rangle=\Sigma_\nu h_\nu|\nu_\alpha\rangle$, and using the expansion of $|\alpha_s\rangle$ in Eq. (3), one can express $C_{\alpha j}=\langle j|\alpha\rangle$ as

$$C_{\alpha j}=\frac{1}{E_\alpha-E_j^0}\sum_\nu\left[\frac{h_\nu}{1-\lambda u_{\alpha\nu}}\langle j|\nu_\alpha\rangle\right](\lambda u_{\alpha\nu})^{m-1}, \tag{8}$$

where m is the smallest positive integer for $\langle j|(Q_{\overline{S}_\alpha}V)^m|\alpha_s\rangle$ not equal to zero [13]. Note that each term in the summation on the right hand side of Eq. (8) decreases exponentially with increasing m, when m is larger than 1. According to the value of m, the set $\overline{S_\alpha}$ can be subdivided into a series of subsets, termed G_m subregions of $\overline{S_\alpha}$, that is, the G_m subregion is composed of those unperturbed states $|j\rangle$ for which $\langle j|(Q_{\overline{S}_\alpha}V)^m|\alpha_s\rangle\neq 0$ and $\langle j|(Q_{\overline{S}_\alpha}V)^n|\alpha_s\rangle=0$ for $n<m$. Since an eigenfunction does not necessarily decrease exponentially inside its G_1 subregion, its main body should generally lie within the region of unperturbed states composed of S_α and the G_1 subregion of $\overline{S_\alpha}$, termed the B_1 region of S_α in what follows.

B. Definition of nonperturbative parts of eigenfunctions

The above results of the GBWPT suggest that it should be useful to divide the eigenfunction of a perturbed state $|\alpha\rangle$ into two parts, termed the perturbative (PT) part and the nonperturbative (NPT) part of the eigenfunction. Correspondingly, the set of unperturbed states is divided into two subsets, termed the PT region and the NPT region of $|\alpha\rangle$, respectively, with the NPT region being a set S_α satisfying the condition (4) and the PT region being the corresponding set $\overline{S_\alpha}$.

Suppose $S_\alpha^{\min}$ is the smallest S_α satisfying the condition (4) and $G_m^{\min}$ is the G_m subregion of $\overline{S}_\alpha^{\min}$. At first sight, Eq. (3) seems to suggest that $S_\alpha^{\min}$ and $\overline{S}_\alpha^{\min}$ should be defined as the NPT and the PT regions of $|\alpha\rangle$, respectively. However, detailed analyses of the $G_1^{\min}$ subregion show that the situation is in fact more complicated. For example, if there is an unperturbed state $|k\rangle$ in $G_1^{\min}$ that is not coupled directly to any of the unperturbed states in $\overline{S}_\alpha^{\min}$ by the perturbation V, then, the perturbation expansion of $C_{\alpha k}$ on the right hand side of Eq. (3) will be truncated with $\langle k|T_\alpha|\alpha_s\rangle$ left only and Eq. (3) will become just the corresponding stationary Schrödinger equation, $\langle k|H|\alpha\rangle=E_\alpha C_{\alpha k}$. Clearly, it is unnecessary to attribute this kind of unperturbed states to the PT region of $|\alpha\rangle$. On the other hand, for unperturbed states $|k\rangle\in G_1^{\min}$ that are coupled to some unperturbed states in $G_2^{\min}$ by V, the values of $C_{\alpha k}$ should be affected by the fact that exponential-type decay begins in the $G_2^{\min}$ subregion. That is, their absolute values, although do not decrease exponentially, may be smaller than those in the $S_\alpha^{\min}$ region, on average, which has indeed been observed in the WBRM model [13]. There is also another problem in defining $S_\alpha^{\min}$ as the NPT region of $|\alpha\rangle$, namely, $S_\alpha^{\min}$ may not be unique and, in practice, it is usually quite difficult to check if a $S_\alpha^{\min}$ obtained numerically is the global minimum.

The definition of the NPT region of a state $|\alpha\rangle$ suggested in this paper is that it includes the unperturbed states in $S_\alpha^{\min}$ and those unperturbed states in $G_1^{\min}$ that are not coupled directly to unperturbed states in $G_2^{\min}$ by the perturbation V. By this definition, the NPT region and the $S_\alpha^{\min}$ region of $|\alpha\rangle$ have the same B_1 region and, as a result, the G_2 subregion of the PT region is just the $G_2^{\min}$ subregion. From the aspect of the GBWPT, there are in fact many possible ways to define the NPT region of $|\alpha\rangle$. A reason for us to take the above one is that, as will be shown numerically below, the NPT parts of eigenfunctions defined in this way may be the largest parts of eigenfunctions having the property that, when the underlying classical system is chaotic, for those NPT parts of eigenfunctions that are sufficiently ergodic, the statistics of their components is in agreement with the prediction of RMT.

In order to check numerically whether this definition of NPT parts of eigenfunctions have the statistical property mentioned above, we employ the Lipkin model, in which there are Ω particles distributed in three orbitals. Here we are interested in their collective motion only. The unperturbed Hamiltonian and the perturbation of the model are taken as (cf. Ref. [23])

$$H_0=\epsilon_0K_{00}+\epsilon_1K_{11}+\epsilon_2K_{22},\quad V=\sum_{t=1}^{4}\mu_tV_t, \tag{9}$$

where

$$V_1=K_{10}K_{10}+K_{01}K_{01},\quad V_2=K_{20}K_{20}+K_{02}K_{02}, \tag{10}$$

$$V_3=K_{21}K_{20}+K_{02}K_{12},\quad V_4=K_{12}K_{10}+K_{01}K_{21}. \tag{11}$$

The operators K_{00}, K_{11}, and K_{22} are particle number operators of the orbitals 0, 1, and 2, respectively, and K_{rs} with $r\neq s$ are the particle raising and lowering operators. In calculation, we took $\Omega=30$ with the dimension of the Hilbert space being 496. The parameters in Eq. (9) were taken as $\epsilon_0=0$, $\epsilon_1\approx 1.47$, $\epsilon_2\approx 2.15$, $\mu_1\approx 0.069$, $\mu_2\approx 0.078$, $\mu_3\approx 0.085$, $\mu_4\approx 0.073$. With these parameters, the strength of the four terms in the perturbation V are comparable with each other. The particle numbers in the three orbitals are good quantum numbers of the unperturbed system H_0. Denoting the particle numbers in the orbitals 1 and 2 by m and n, respectively, the particle number in the orbital 0 is $\Omega-m-n$. Using m and n, the unperturbed state $|k\rangle$ is labeled by $|mn\rangle$. For this model, the condition (4) can be satisfied, when $|E_\alpha-E_k^0|$ is large enough for each of the unperturbed states $|k\rangle$ in $\overline{S_\alpha}$.

In the calculation of $S_\alpha^{\min}$, one should note that $E_{mn}^0=\epsilon_1m+\epsilon_2n$ and the perturbation V couples unperturbed states with $|\Delta m|$ and $|\Delta n|$ less than 3 only. In practice, we

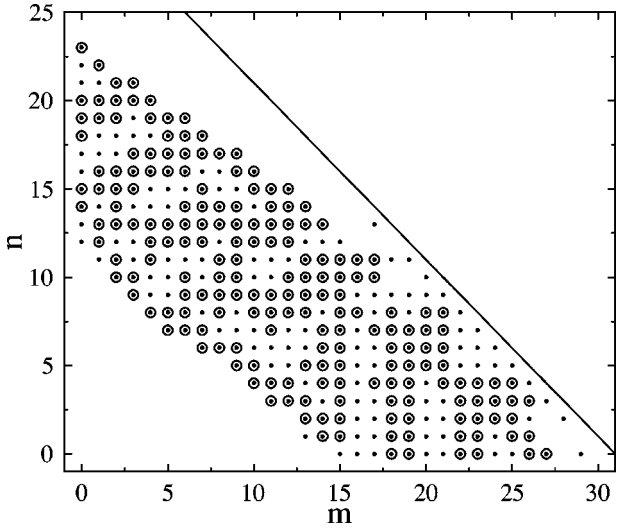

FIG. 1. Dots and circles indicate the positions of the unperturbed states $|mn\rangle$ in the nonperturbative region of the state $|\alpha=260\rangle$ and those in a locally minimum $S_\alpha^{\min}$ region, respectively, when $\lambda=0.6$. The solid straight line is the line of $m+n=\Omega+1$.

first calculate an intermediate S_α, denoted by $S_\alpha^{\rm im}$, in the following way: (i) Starting from a set S_α including all the unperturbed states, for each n, we move states $|mn\rangle$ to the set $\overline{S_\alpha}$ with m first decreasing from the largest value (Ω here), then increasing from the smallest value (zero here), until the condition (7) is not satisfied; (ii) for the set S_α obtained, for each m, we do the same thing as having been done for n. In the second step, we try to move out each of the states $|mn\rangle$ in the set $S_\alpha^{\rm im}$ to see if the condition (7) is still satisfied and finally obtain a $S_\alpha^{\min}$. In numerical calculation, denoting $\langle\phi|(T_\alpha^\dagger)^n T_\alpha^n|\phi\rangle$ as X_n with $|\phi\rangle$ being a normalized vector chosen arbitrarily, Eq. (7) was treated in the way that (a) it is regarded as correct, if $X_n<10^{-6}$ when $n<10^4$, or $X_n<X_{n-1000}$ when $n=10^4$; (b) it is taken as incorrect, if $X_n>1000$ when $n<10^4$, or $X_n>X_{n-1000}$ when $n=10^4$. Numerically, the same NPT regions have been obtained in different ways of trying to move out unperturbed states in $S_\alpha^{\rm im}$, which usually give different $S_\alpha^{\min}$ regions (see Fig. 1 for an example). Numerical calculations show that good approximations to NPT regions of perturbed states can in fact be obtained by using $S_\alpha^{\rm im}$ in place of $S_\alpha^{\min}$, the calculation time of which is much shorter.

To study statistical properties of NPT parts of eigenfunctions that are sufficiently ergodic, we make use of their relative localization length R_α. Denoting the normalized values of $w_{mn}=|\langle mn|\alpha\rangle|^2$ in the NPT region of $|\alpha\rangle$ with N_α unperturbed states by w'_{mn}, namely, $w'_{mn}=w_{mn}/A$, where $A=\Sigma_{\rm NPT} w_{mn}$ with the summation over the unperturbed states in the NPT region of $|\alpha\rangle$, R_α is defined by $R_\alpha=C_\alpha^N/C_{GOE}$, where

$$C_\alpha^N=\exp\left(-\sum_{\rm NPT} w'_{mn}\ln w'_{mn}\right) \tag{12}$$

and $C_{GOE}\approx N_\alpha/2.07$ is the prediction of RMT for the Gaussian orthogonal ensemble (GOE) of N_α-dimensional random matrices. For NPT parts of eigenfunctions satisfying $|R_\alpha-1|<0.02$, where $151\leqslant\alpha\leqslant350$ and $\lambda=0.5,0.6,\ldots,1.0$, the distribution of their components, denoted by $f(x)$, has been found in good agreement with the prediction of GOE for M-dimensional matrices in the limit $M\to\infty$,

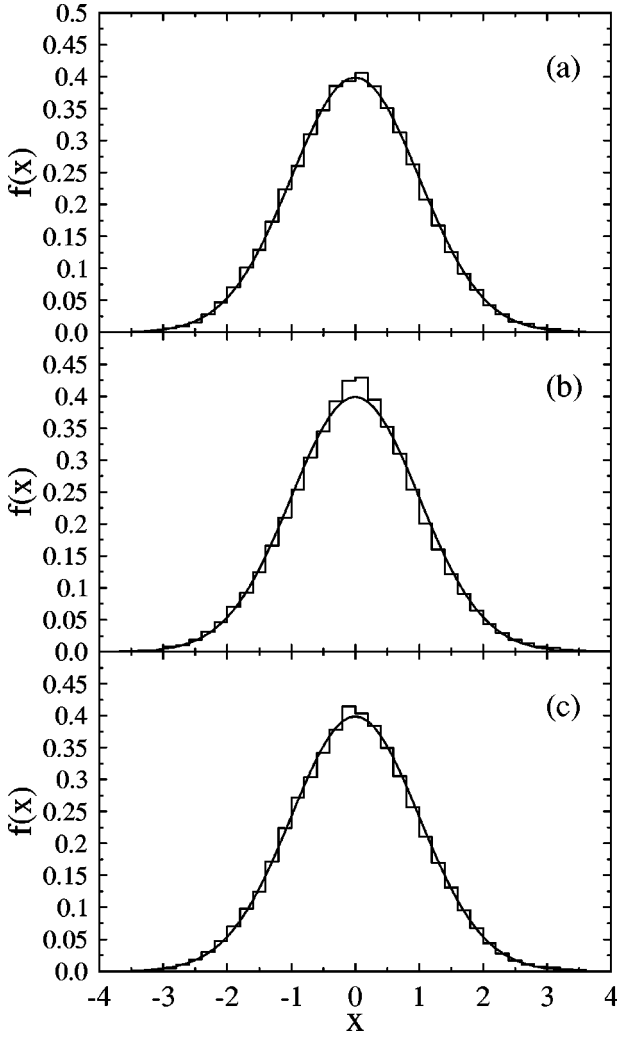

FIG. 2. (a) The histogram of the distribution of components in the nonperturbative parts of eigenfunctions whose relative localization length R_α are close to 1. Total 53 832 components were used in the calculation of the histogram. The solid curve is the Gaussian distribution predicted by GOE. (b) Same as in (a) for the distribution of components in the B_1 regions of the nonperturbative regions (81 499 components used). (c) Same as in (a) for the distribution of components in S_α^e regions (65 905 components used).

$$f_{GOE}(x)=\frac{1}{\sqrt{2\pi}}\exp(-x^2/2), \tag{13}$$

where $x=C_{\beta i}\sqrt{M}$ with $C_{\beta i}$ being components of the eigenfunctions of the random matrices [2] [Fig. 2(a)]. In the calculation of $f(x)$, since different eigenfunctions may have different numbers of components in their NPT parts and the average absolute values of components in cases of different λ are different, we first put components of the eigenfunctions

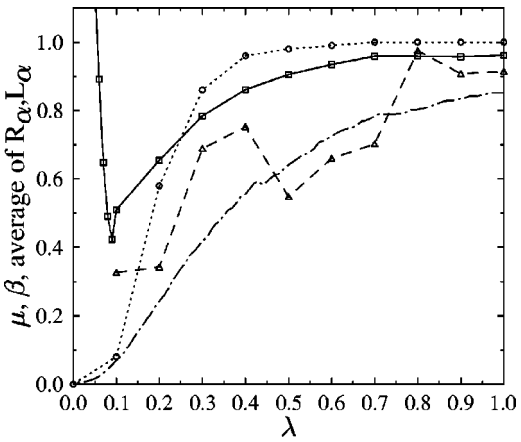

FIG. 3. Variation of $\overline{R}$, the average relative localization length of nonperturbative parts of eigenfunctions in the middle of energy region ($\alpha=186$–310) (squares connected by solid line). Together we show the values of μ (circles connected by dotted line), the Brody parameter β (triangles connected by dashed line), and $\overline{L}$ (dashed-dotted curve) in the same energy region.

of the same λ together and normalize them, then, put data of different λ together and normalize them again.

The requirement that $|R_\alpha-1|<0.02$ itself does not guarantee the closeness between the statistics of the NPT parts of the eigenfunctions and the prediction of RMT. For example, similar to R_α, one can introduce relative localization length in the B_1 regions of NPT regions, denoted by R^b_α. For those B_1 regions satisfying $|R^b_\alpha-1|<0.02$, the distribution of their components has been found higher than $f_{GOE}(x)$ in the small component region [see Fig. 3(b)]. This means that the absolute values of the components in the G_1 subregions of the PT regions are smaller than those inside the NPT regions, on average, which has also been observed numerically in the WBRM model [13,35]. In fact, the statistics of components in some regions smaller than the B_1 regions has also been found to deviate from $f_{GOE}(x)$. For example, consider the smallest $S_\alpha=\{|k\rangle:k=p_1,p_1+1,\ldots,p_2\}$ satisfying the condition (4), denoted by S^e_α, which were used in Ref. [13]. Similar to the case of B_1 regions, we have calculated the distribution of components in those S^e_α regions whose relative localization length R^e_α is close to 1, and have found a small deviation from the form of $f_{GOE}(x)$ in the small x region [Fig. 3(c)]. Numerically, S^e_α regions have been found usually a little larger than the corresponding NPT regions.

III. NONPERTURBATIVE AND PERTURBATIVE PARTS OF EIGENFUNCTIONS

In this section, we study properties of NPT and PT parts of eigenfunctions, when the underlying classical system undergoes a crossover from integrability to chaos. In Sec. III A, we discuss numerical results obtained in the middle of energy region. Some properties of eigenfunctions manifested in the variation of localization length are discussed in Sec. III B.

A. Structure of eigenfunctions and their NPT regions

When the parameter λ increases from zero, the integrability of the classical counterpart of the Lipkin model will be destroyed gradually. A measure of the destruction is given by the fraction of chaotic volume in phase space denoted by μ. Figure 3 shows the variation of μ with λ in the energy region between the perturbed energies E_{186} and E_{310} of the corresponding quantum system. The values of μ was calculated by making use of Monte Carlo methods, in the same way as in Ref. [7]. Together, in Fig. 3, we show the variation of the Brody parameter β, which were obtained by the best fitting of the cumulative form of the Brody distribution $p_B(s,\beta)$ to the cumulative nearest-level-spacing distribution $\int_0^s p(x)dx$ in the corresponding energy region, where

$$p_B(s,\beta)=As^\beta\exp(-Bs^{1+\beta}), \tag{14}$$

$$A=(1+\beta)B, \quad B=\Gamma^{1+\beta}\left(\frac{2+\beta}{1+\beta}\right). \tag{15}$$

To obtain a better statistics, we have used data obtained from ten values of $H(\lambda')$ with λ' close to λ ($\delta\lambda<0.025$). We see that the variation of β is quite irregular and, when λ is between 0.6 and 0.7, the values of β are quite lower than $\mu\approx1.0$. The cumulative nearest-level-spacing distributions of $\lambda=0.4$, 0.6, and 0.8 are presented in Fig. 4, in comparison with the prediction of the Wigner surmise [3] (dotted curves), $p_W(s)=(\pi s/2)\exp(-\pi s^2/4)$, and the best fitting cumulative Brody distributions (dashed curves).

The average of relative localization length R_α of NPT parts of eigenfunctions, denoted by $\overline{R}$, can be used to characterize the behavior of the quantum system in the process of the underlying classical system changing from an integrable system to a chaotic one. Variation of $\overline{R}$ with λ, with average taken over the states of $\alpha=186$–310, is shown in Fig. 3 by

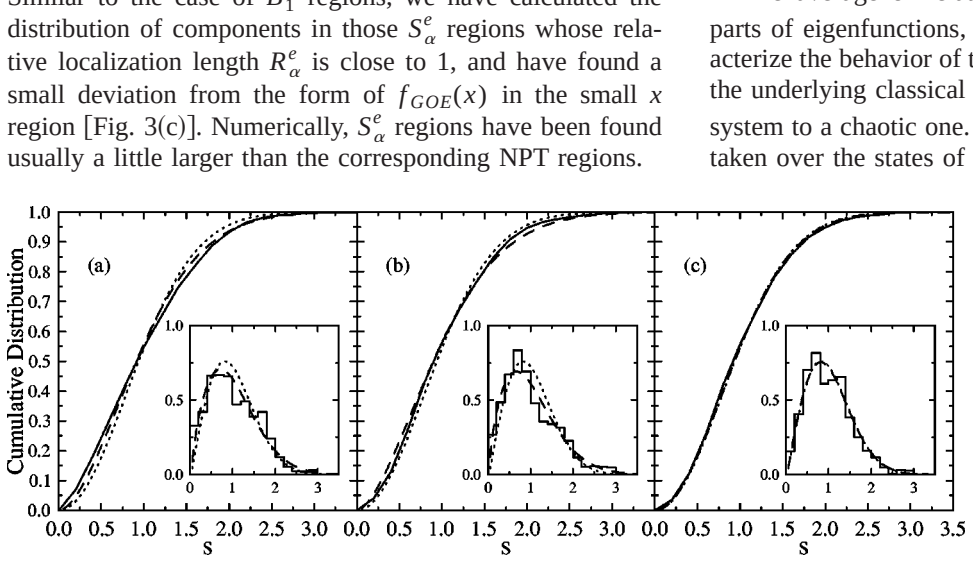

FIG. 4. Cumulative nearest-level-spacing distributions in the middle of energy region (solid curves); (a) $\lambda=0.4$, (b) $\lambda=0.6$, and (c) $\lambda=0.8$. The nearest-level-spacing distributions themselves are shown in the insets. The prediction of Wigner surmise are given by dotted curves and the best fitting Brody distributions and their cumulative forms are shown by dashed curves.

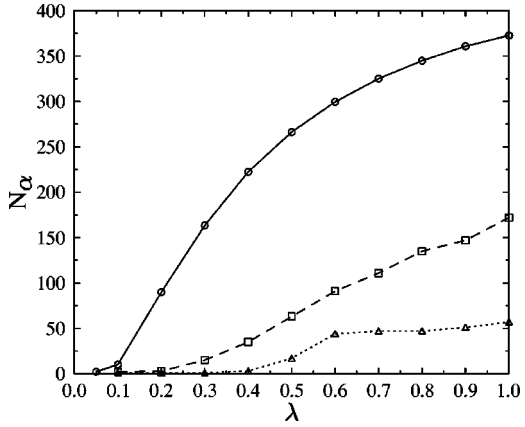

FIG. 5. Variation of $\langle N_\alpha \rangle$, the average number of unperturbed states in the nonperturbative regions of perturbed states in the middle of energy region ($\alpha = 151$–350) (circles connected by solid curve). Triangles (connected by dotted line) and squares (connected by dashed line) show the values of N_α for the ground state and the ninth excited state ($\alpha = 10$), respectively.

squares connected by solid line. We see that $\overline{R}$ becomes almost saturated and close to μ, when λ is larger than 0.7. The behavior of $\overline{R}$ is obviously more regular than β. For λ between 0.2 and 0.7, the values of μ are closer to $\overline{R}$ than to β. (The behavior of β has been found more regular, when either the energy region is enlarged or the particle number Ω is increased to 40 so that more energy levels are taken into account. But, in both cases, the behavior of β has been found still more irregular than $\overline{R}$ and the values of β in the parameter regime $0.6 \leqslant \lambda \leqslant 0.7$ obviously smaller than $\overline{R}$ as well.) For comparison, Fig. 3 also gives the variation of $\overline{L} = \langle L_\alpha \rangle$, the average of the relative localization length of the whole eigenfunctions defined in the ordinary way.

Now let us discuss detailed properties of NPT parts of eigenfunctions in the middle of energy region. When the perturbation is sufficiently weak, the ordinary perturbation theory works and the NPT region of a perturbed state $|\alpha\rangle$ is just the unperturbed state $|k\rangle$ of $k = \alpha$. In this case, $R_\alpha \approx 2.07$. With increasing λ, the sizes of both the NPT regions and the main bodies of eigenfunctions will enlarge. Figure 3 shows that the increasing of $\overline{R}$ starts at $\lambda \approx 0.09$. The variation of $\langle N_\alpha \rangle$ is given in Fig. 5. Numerically, for a fixed λ, perturbed states with similar energies have been found having NPT regions with qualitatively similar structures.

Examples of the shapes of NPT regions and their B_1 regions of $|\alpha = 260\rangle$ in cases of λ from 0.05 to 0.7 are given in Fig. 6, with the main bodies of the eigenfunctions shown schematically by crosses. In Fig. 6(b), the NPT region is roughly along a slanted straight line with a slope close to $-2/3$. This is because the energies of the unperturbed states $|mn\rangle$ in the NPT region are close to E_{260} with $\epsilon_1/\epsilon_2 \approx 2/3$. When the classical system is mixed, eigenfunctions have been found composed of three parts, namely, main bodies localized in their B_1 regions, tails inside the B_1 regions with relatively slow decaying speed, and tails outside of the B_1 regions with relatively fast decaying speed. The phenomenon that the main bodies do not occupy the full NPT regions is related to the fact that the GBWPT, derived from the eigenequation of energy, does not consider the destruction of the other conserved quantities of H_0. As to the behavior of eigenfunctions outside of the B_1 regions, as predicted by the GBWPT, exponential-type decay has been found, on average (Fig. 7). Eigenfunctions ergodic or almost ergodic in their NPT regions have also been found, whose eigenenergies are in avoided-level-crossing regions.

In the case of the classical system being almost chaotic, namely, $\lambda \geqslant 0.5$, most of the eigenfunctions have been found ergodic or almost ergodic in their NPT regions, with $\overline{R}$ larger than 0.9 (Fig. 3). In agreement with the feature of $f(x)$ at small x shown in Fig. 2(b), for eigenfunctions of $\lambda \geqslant 0.5$, the values of w_{mn} in the G_1 subregions of their PT regions have been found smaller than those in their NPT regions, on average. Meanwhile, there are also some eigenfunctions not fully ergodic in their NPT regions, with large components in the small n, or small m, or $m+n \approx \Omega$ region(s), such as the

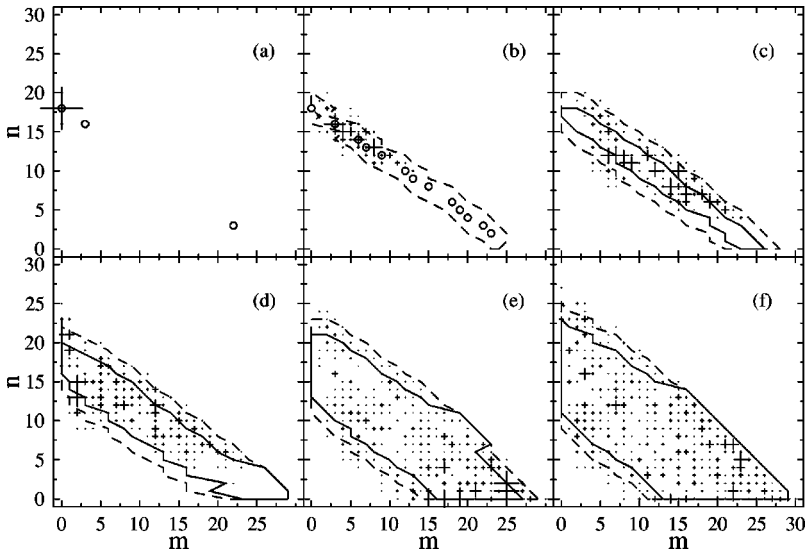

FIG. 6. Nonperturbative regions of the perturbed states $|\alpha = 260\rangle$ in cases of different perturbation parameter λ, (a) $\lambda = 0.05$, (b) $\lambda = 0.1$, (c) $\lambda = 0.2$, (d) $\lambda = 0.3$, (e) $\lambda = 0.5$, and (f) $\lambda = 0.7$. Circles in (a) and (b) indicate positions of the unperturbed states $|mn\rangle$ in the nonperturbative regions. Solid and dashed curves in (b)–(f) show the rough boundaries of the nonperturbative regions and their B_1 regions, respectively. The main bodies of the eigenfunctions are shown schematically by crosses. Length of the crosses, with centers at (m,n), are proportional to $w_{mn} = |\langle mn|\alpha\rangle|^2$. For the eigenfunctions in (a)–(f), $s_w = \Sigma_{\text{cross}} w_{mn} \approx 0.97$.

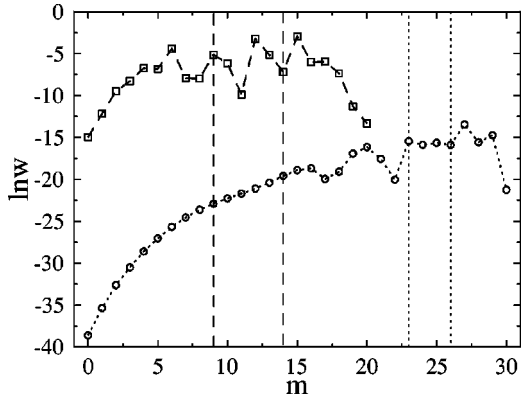

FIG. 7. The values of $\ln w_{mn}$ with $n=0$ (circles connected by dotted line) and with $n=10$ (squares connected by dashed line) for the eigenfunction shown in Fig. 6(c). The vertical dotted straight lines and dashed straight lines show the boundaries of the nonperturbative region in the corresponding cases, respectively.

one shown in Fig. 6(e), which make $\overline{R}$ less than 1. To understand this phenomenon, we have studied the values of v_t^{mn},

$$v_t^{mn}=\sum_{m'n'}\langle m'n'|\mu_t V_t|mn\rangle, \tag{16}$$

which are plotted schematically by the length of the crosses in Fig. 8. We see that the perturbation V has relatively small elements in the $m+n\approx\Omega$ region and only one of its four terms has large elements in the small m or small n region.

Nonperturbative regions of low lying states have features different from those in the middle of energy region. For example, since E_1 is lower than E_1^0 and the distance $|E_1-E_1^0|$ increases with increasing λ, the sizes of the NPT regions of perturbed ground states are much smaller than those in the middle of energy region. An interesting feature of the NPT regions of perturbed ground states of $\lambda\geqslant 0.5$ is that they move to some regions above the point (0,0) in the (m,n) plane, which is due to the fact that the values of $|E_1-E_1^0|$ are large for large λ and the elements of the perturbation V are relatively small in the neighborhood of (0,0) (see Fig. 8). Variation of the sizes of NPT regions of $\alpha=1$ and 10 with λ are also shown in Fig. 5.

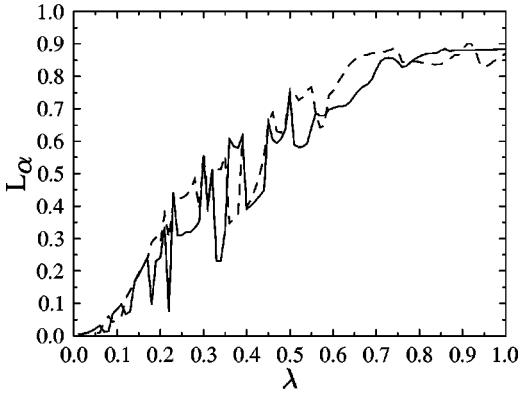

FIG. 9. Variation of L_α, the relative localization length of whole eigenfunctions, with λ for $\alpha=203$ (solid curve) and $\alpha=204$ (dashed curve).

B. Some features of eigenfunctions manifested in the variation of relative localization length

Some features of eigenfunctions can be seen in the variation of their relative localization length L_α with the perturbation parameter λ. Two examples are given in Fig. 9, which show large fluctuations of L_α due to the ''exchange'' of states in avoided-level-crossing (ALC) regions. Detailed variation of L_α and R_α in the parameter regime $0.2\leqslant\lambda\leqslant 0.5$ are shown in Figs. 10(b) and 10(c), respectively. Comparing with the variation of eigenenergies shown in Fig. 10(a), we see that peaks of L_α and R_α indeed correspond to ALC regions. Figure 10(b) shows that the value of L_α usually increases steadily outside of ALC regions.

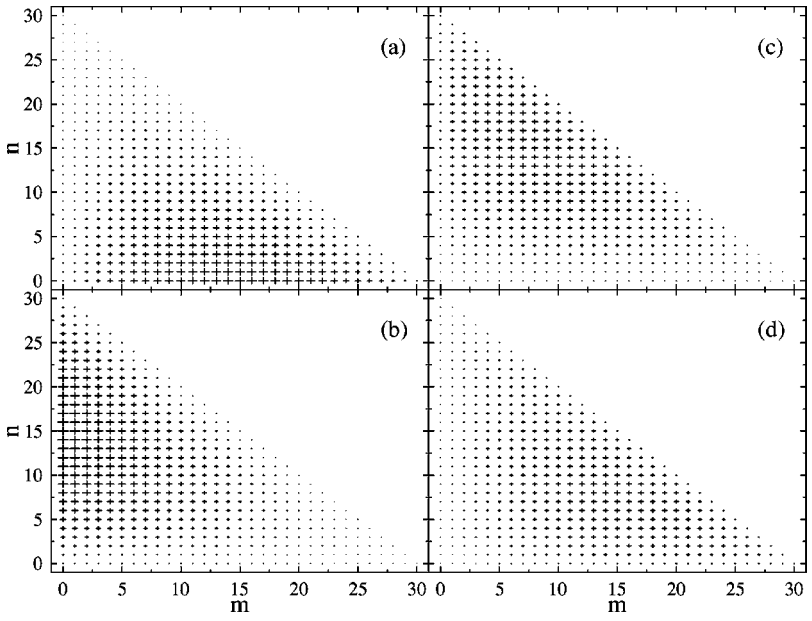

FIG. 8. Length of the crosses at (m,n) are proportional to v_t^{mn} in Eq. (16); (a) $t=1$, (b) $t=2$, (c) $t=3$, and (d) $t=4$.

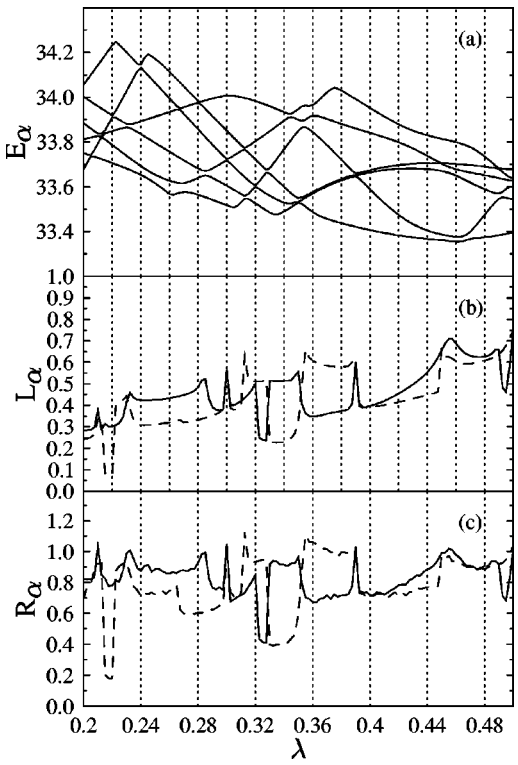

FIG. 10. (a) Variation of E_α with λ ($\alpha=201-206$). (b) Variation of L_α with λ for $\alpha=203$ (solid curve) and $\alpha=204$ (dashed curve). (c) Same as (b) for R_α.

Figure 10(c) shows that the values of R_α at some of the peaks exceed 1, e.g., the one at $\lambda\approx0.3$, i.e., ALC can induce ''ergodicity'' of eigenfunctions. To show this phenomenon more clearly, in Fig. 11 we show the main bodies of the eigenfunctions of $\alpha=203$ and 204 before, at, and after the ALC at $\lambda\approx0.3$, respectively, together with the corresponding NPT and B_1 regions. The mixing and separation of the main bodies of the two eigenfunctions can be seen quite clearly, with positions exchanged after the ALC. Figures 10(b) and 10(c) show that there are also some eigenfunctions whose L_α and R_α are relatively small compared with the other levels of the same λ, e.g., the R_{203} in the neighborhood of $\lambda=0.325$. For such eigenfunctions, it has been found that their largest components usually lie in the (m,n) regions where the perturbation matrix elements are relatively small.

IV. CONCLUSIONS AND DISCUSSIONS

In this paper, we have studied nonperturbative and perturbative parts of energy eigenfunctions in a schematic shell model, when the underlying classical system undergoes a transition from integrability to chaos. We have introduced a definition of nonperturbative parts of eigenfunctions, with the corresponding perturbative parts expanded in a convergent perturbation expansion by making use of the nonperturbative parts. The nonperturbative parts have been shown to have the property that, when the underlying classical system is chaotic, for those nonperturbative parts of eigenfunctions whose relative localization length are close to 1, the statistics of their components is in agreement with the prediction of random-matrix theory.

Nonperturbative parts of eigenfunctions in different perturbation parameter regimes have been studied numerically. With increasing perturbation parameter, sizes of the nonperturbative parts have been found to increase, with the main bodies of the eigenfunctions usually lying within the B_1 regions of their nonperturbative regions in the whole perturbation parameter regime, and within their nonperturbative regions when perturbation is not weak. When the underlying classical system is mixed, most of the eigenfunctions have been found to be composed of three parts, roughly speaking, main bodies localized in the nonperturbative/B_1 regions, tails inside the nonperturbative/B_1 regions, and tails outside the nonperturbative/B_1 regions; meanwhile, some of the eigenfunctions have been found ergodic in their nonperturbative regions due to avoided level crossings. When the classical system becomes chaotic, most of the eigenfunctions have been found ergodic or almost ergodic in their nonperturbative regions. Numerical results show that the average relative localization length of nonperturbative parts of eigenfunctions is useful in characterizing the behavior of the quantum system, in the process of the underlying classical system changing from a mixed system to a chaotic one.

Numerical results presented in this paper show that the division of eigenfunctions into perturbative and nonperturbative parts is indeed useful in revealing interesting properties

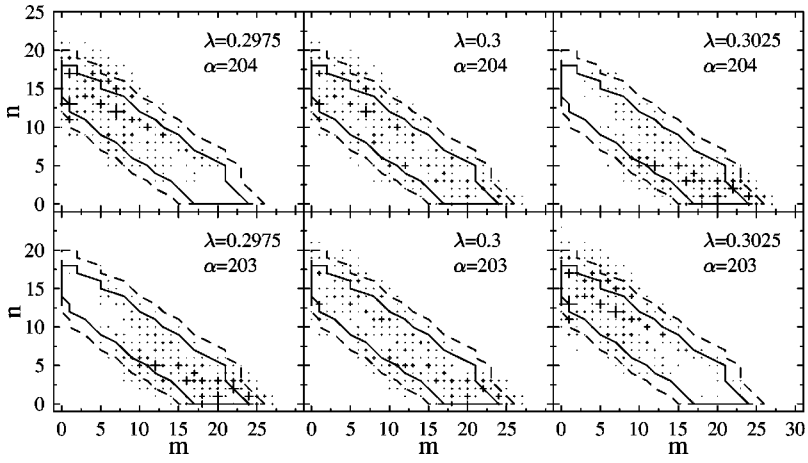

FIG. 11. Schematic plot (by crosses) of the main bodies of the eigenfunctions of $\alpha=203$ and 204, with respect to their nonperturbative regions and the corresponding B_1 regions, before and after the avoided level crossing at $\lambda\approx0.3$ in (a).

of the eigenfunctions. The numerical calculation of the division is somewhat time consuming. However, when approximate results are required only, the calculation time can be reduced considerably by, for example, making use of the intermediate regions discussed in Sec. II of this paper. An analytical study of the convergence condition in the GBWPT may reduce the calculation time as well. Although the definition of the division adopted in this paper is better than the one used previously, it is possibly not the final one, since the separation of the $G_1^{\min}$ subregion into its subperturbative and subnonperturbative parts is not made completely from general requirements, but, in fact, to some extent from numerical results obtained. A possible improvement of the definition may be including all the locally minimal $S_\alpha^{\min}$ regions, the calculation time of which would be considerably long.

Properties of nonperturbative parts of energy eigenfunctions have been studied in a specific model with a finite Hilbert space in this paper. Since the convergence condition for the perturbative parts of eigenfunctions can always be satisfied when the corresponding nonperturbative parts are taken large enough, separation of eigenfunctions into perturbative and nonperturbative parts can be made in an arbitrary system, even when the Hilbert space is infinite. The problem is how much useful information the separation could supply. In fact, for some systems with infinite Hilbert spaces, e.g., the quartic anharmonic oscillator, the separation does not supply as much information as in the case of finite Hilbert space. For such systems, in order to obtain more useful information, the present form of the GBWPT should by modified, which needs further research work.

ACKNOWLEDGMENTS

The author is grateful to P. A. Braun for valuable discussions. Support from the Natural Science Foundation of China is gratefully acknowledged.

[1] B. Eckhardt, Phys. Rep. **163**, 205 (1987).
[2] F. Haake, *Quantum Signatures of Chaos*, 2nd ed. (Springer-Verlag, Berlin, 2001).
[3] O. Bohigas, in *Chaos and Quantum Physics*, Proceedings of the Les Houches Summer School, Session LII, edited by M.-J. Giannoni, A. Voros, and J. Zinn-Justin (North-Holland, Amsterdam, 1991).
[4] *Quantum Chaos: Between Order and Disorder*, edited by G. Casati and B. V. Chirikov (Cambridge University Press, Cambridge, UK, 1994).
[5] B. Li and M. Robnik, J. Phys. A **27**, 5509 (1994); **28**, 2799 (1995); A. Kudrolli, V. Kidambi, and S. Sridhar, Phys. Rev. Lett. **75**, 822 (1995).
[6] K. Müller, B. Mehlig, F. Milde, and M. Schreiber, Phys. Rev. Lett. **78**, 215 (1997).
[7] D. C. Meredith, S. E. Koonin, and M. R. Zirnbauer, Phys. Rev. A **37**, 3499 (1988).
[8] V. V. Flambaum, A. A. Gribakina, G. F. Gribakina, G. F. Gribakin, and M. G. Kozlov, Phys. Rev. A **50**, 267 (1994); V. V. Flambaum, G. F. Gribakin, and F. M. Izrailev, Phys. Rev. E **53**, 5729 (1996).
[9] D. Cohen, Phys. Rev. Lett. **82**, 4951 (1999); D. Cohen and E. Heller, *ibid.* **84**, 2841 (2000).
[10] M. Mehta, *Random Matrices*, 2nd ed. (Academic Press, New York, 1991).
[11] T. Guhr, A. Müller-Groeling, and H. A. Weidenmüller, Phys. Rep. **299**, 189 (1998).
[12] G. Casati, B. V. Chirikov, I. Guarneri, and F. M. Izrailev, Phys. Lett. A **223**, 430 (1996).
[13] Wen-ge Wang, Phys. Rev. E **61**, 952 (2000); Commun. Theor. Phys. **35**, 143 (2001).
[14] G. Casati, B. V. Chirikov, J. Ford, and F. M. Izrailev, Lect. Notes Phys. **93**, 334 (1979).
[15] F. Borgonovi, G. Casati, and B. Li, Phys. Rev. Lett. **77**, 4744 (1996).
[16] K. Frahm and D. L. Shepelyansky, Phys. Rev. Lett. **78**, 1440 (1997); **79**, 1833 (1997).
[17] F. Borgonovi, Phys. Rev. Lett. **80**, 4653 (1998).
[18] G. Casati and T. Prosen, Phys. Rev. E **59**, R2516 (1999).
[19] H. Friedrich and D. Wintgen, Phys. Rep. **183**, 37 (1989).
[20] M. C. Gutzwiller, *Chaos in Classical and Quantum Mechanics* (Springer, New York, 1990).
[21] T. Guhr, Phys. Rev. Lett. **76**, 2258 (1996).
[22] K. Karremans, W. Vassen, and W. Hogervorst, Phys. Rev. Lett. **81**, 4843 (1998).
[23] Wen-ge Wang, F. M. Izrailev, and G. Casati, Phys. Rev. E **57**, 323 (1998).
[24] F. Borgonovi, I. Guarneri, and F. M. Izrailev, Phys. Rev. E **57**, 5291 (1998).
[25] T. Prosen and M. Robnik, J. Phys. A **26**, L319 (1993); **26**, 1105 (1993).
[26] T. Prosen, Ann. Phys. (N.Y.) **235**, 115 (1994).
[27] D. Boosé and J. Main, Phys. Rev. E **60**, 2831 (1999).
[28] T. Brody *et al.*, Rev. Mod. Phys. **53**, 385 (1981).
[29] M. V. Berry and M. Robnik, J. Phys. A **17**, 2413 (1984).
[30] F. M. Izrailev, Phys. Lett. A **125**, 250 (1987); **134**, 13 (1988).
[31] E. Wigner, Ann. Math. **62**, 548 (1955); **65**, 203 (1957).
[32] Wen-ge Wang, Phys. Rev. E **63**, 036215 (2001).
[33] H. J. Lipkin, N. Meshkov, and A. J. Glick, Nucl. Phys. **62**, 188 (1965).
[34] Xu Gong-ou, Gong Jiang-bin, Wang Wen-ge, Yang Ya-tian, and Fu De-ji, Phys. Rev. E **51**, 1770 (1995).
[35] In the case of the Wigner-band random-matrix model, the definition of NPT regions of perturbed states given in this paper is consistent with the one used in Ref. [13].